

Evaluation of Digital Speckle Filters for Ultrasound Images

Fara Nabila Radzi¹, Norashikin Yahya²

Department of Electrical and Electronic Engineering Universiti Teknologi PETRONAS
Tronoh, Malaysia

fararadzi91@gmail.com¹, norashikin_yahya@petronas.com.my²

Abstract—Ultrasound (US) images are inherently corrupted by speckle noise causing inaccuracy of medical diagnosis using this technique. Hence, numerous despeckling filters are used to denoise US images. However most of the despeckling techniques cause blurring to the US images. In this work, four filters namely Lee, Wavelet Linear Minimum Mean Square Error (LMMSE), Speckle-reduction Anisotropic Diffusion (SRAD) and Non-local-means (NLM) filters are evaluated in terms of their ability in noise removal. This is done through calculating four performance metrics Peak Signal to Noise Ratio (PSNR), Ultrasound Despeckling Assessment Index (USDSAI), Normalized Variance and Mean Preservation. The experiments were conducted on three different types of images which is simulated noise images, computer generated image and real US images. The evaluation in terms of PSNR, USDSAI, Normalized Variance and Mean Preservation shows that NLM filter is the best filter in all scenarios considering both speckle noise suppression and image restoration however with quite slow processing time. It may not be the best option of filter if speed is the priority during the image processing. Wavelet LMMSE filter is the next best performing filter after NLM filter with faster speed.

Keywords—Ultrasound images, Despeckling, denoise, LMMSE, SRAD, NLM, PSNR, USDSAI

I. INTRODUCTION

Application of ultrasound (US) in medicine began as early as during the Second World War and has been developing rapidly ever since [1]. Ultrasound imaging is a very essential technique in medical diagnosis due to its safe, economical and non-invasive nature. Technically, ultrasound images are formed from the echo signals that are reflected back to the transducers from the tissues or organs [2]. These echoes are formed through two processes, namely scattering and specular reflection. Scattering gives rise to overlapping echoes that undergo a phenomenon called interference which results in speckle being formed [3]. Therefore it can be said that US images are inherently corrupted with speckle, a form of noise which attenuates US images qualities, causing image interpretation and processing a tough task. Speckle can be characterized as irregular coarse patterns of spots. They reduce US image contrast causing difficulties in deriving useful information for both non-specialists and experts. Hence, there are many efforts made by researches to formulate various despeckling methods for denoising US images. Speckle is modeled as an accumulation of a large number of complex phasors. Specifically, in amplitude format, speckle is also known as complex random walk following the Rayleigh distribution given as

$$P_A(A) = \frac{A}{v^2} \exp\left(-\frac{A^2}{2v^2}\right), \quad A \geq 0 \quad (1)$$

where v^2 is the variance of the Gaussian distributed in-phase/quadrature (IQ) components. The noisy US image, $z(i,j)$ is modeled as

$$z(i,j) = x(i,j) \cdot n(i,j) + g(i,j), \quad (2)$$

where $x(i,j)$ represents noise-free pixel, $n(i,j)$ and $g(i,j)$ represents multiplicative and additive noise, respectively. Meanwhile, i and j represent the rows and columns in 2-D image. However, since the effect of additive noise is significantly smaller than multiplicative noise and can be assumed negligible, equation (2) can be re-written as

$$z(i,j) \approx x(i,j) \cdot n(i,j), \quad (3)$$

which makes speckle noise modeled as purely multiplicative. After log transform, the speckle adopts the form of

$$\log(z(i,j)) = \log(x(i,j)) + \log(n(i,j)), \quad (4)$$

and can be simplified to

$$z_l(i,j) = x_l(i,j) + n_l(i,j). \quad (5)$$

This paper is organized as follows. Section II gives a brief description of the selected despeckling filters. Section III presents the performance metrics used to evaluate the speckle filters. Section IV presents the results and discussions. In particular, the results presented in section IV are using 3 type of images, 1) using image corrupted by simulated speckle noise, 2) using Field II generated image and 3) using real US images. Lastly, section V concludes the paper.

II. DESPECKLING FILTERS

There are various filters that have been derived by the researches that aim to remove the speckle and at the same time enhance the contrast while preserving the edges of the US images [4]. These filters can be categorized according to their types such as linear spatial adaptive, wavelet, non-local means and diffusion. Some of the common filters are Lee, Kuan, Frost [7], Homomorphic [8], anisotropic diffusion [9], SRAD

[10], wavelet LMMSE [11] and NLM [12]. In this study, the filters to be evaluated are chosen from respective categories and they are Lee, wavelet (LMMSE), NLM and SRAD.

Lee filter utilizes local statistics to perform edge preservation [5]. Edges are assumed to have high variance and therefore areas with high variance will not be smoothed meanwhile areas with less variance will be smoothed [13]. Since Lee filter is based on first order statistical model, its performance is greatly affected by the window size and shape [13].

The wavelet (LMMSE) Filter proposed by Zhang and Bao this filter is a LMMSE-based with optimal wavelet selection filter. The pioneer wavelet soft thresholding concept was proposed by Donoho, and afterwards followed by many other wavelet-based methods such as in [14], [15], and [16]. The method utilized the interscale model and presented using overcomplete wavelet expansion (OWE). Wavelet filters must have two characteristics in order to perform denoising which is the ability to extract signals from noisy wavelet coefficient and another is the resemblance of interscale image wavelet coefficients distributions to jointly Gaussian. The common despeckling steps with wavelets are the computation of wavelet transform, removal of speckle noise from wavelet coefficients and reconstruction of the despeckled images [17].

Non-local means filter uses non-local pixels in the filtering process. This is different than the concept of previous filters which are all based on local relevant pixels. Proposed by Buades in [12] this filter uses the approach of comparing non-local patches and filtering is conducted based on their similarity [18]. This is called the self-similarity concept which was first introduced by Efros and Leung [19].

The SRAD filter is capable of removing speckle without eliminating image information and also preserves edges [20]. Proposed by Yongjian and Acton [10], SRAD filter is an extension of AD filter by Perona and Malik in [9], aimed at being more efficient in speckle removing. It still operates based on diffusion PDE like AD filter but additionally utilizes instantaneous coefficient of variation (ICOV) [21].

III. PERFORMANCE METRICS

In this work, four performance metrics are utilized namely PSNR, USDSAI, Mean Preservation and Normalized Variance. The following sub-sections discuss the selected performance metrics:

- 1) *Peak Signal to Noise Ratio (PSNR)*: gives a ratio of maximum power of signal to the noise level where MSE is the mean square error

$$PSNR = 20 \log_{10} \left(\frac{255}{\sqrt{MSE}} \right), \quad (6)$$

- 2) *Mean Preservation*: The mean before and after denoising is compared whereby better filter will result in mean intensity closer to original image's mean [25].

$$\bar{X} = \frac{1}{MN} \sum_{i=1}^M \sum_{k=1}^N X_{j,k} \quad (7)$$

- 3) *Normalized Variance*: Lower normalized variance signifies better speckle reduction and it is expressed as

$$\frac{var}{mean^2} = \frac{\frac{1}{MN} \sum_{j=1}^M \sum_{k=1}^N (X_{j,k} - \bar{X})^2}{\bar{X}^2} \quad (8)$$

where \bar{X} is the mean of $M \times N$ pixels image size [25].

- 4) *Ultrasound Despeckling Assessment Index (USDSAI)*: USDSAI measures the speckle filters' performance in terms of reduction in variances of homogenous regions while separating the different regions apart [25].

$$USDSAI = \frac{\sum_{k \neq l} mean_{c_k} - mean_{c_l}}{variance_{c_k}} \quad (9)$$

IV. RESULTS AND DISCUSSIONS

A. Using Simulated Noise Speckled Images

In this section, the results of PSNR and USDSAI evaluations on the despeckled simulated noisy images are disclosed. Three images Lena, Barbara and Boat are used in the experiment of PSNR and USDSAI evaluations. The 128×128 pixels clean images are introduced with simulated speckle noise of varying noise variance levels. The comparison of PSNR and USDSAI values are summarized in Table I and II respectively.

From Table 1, it is evident that wavelet (LMMSE) is the most superior despeckling technique with consistently highest PSNR values for Lena and Boat images. It has the highest average gain of PSNR with both these images. In Barbara image it is seen that NLM filter performs best from noise variances 0.04 up to 0.1 and wavelet LMMSE is observed to have highest PSNR from noise variances 0.2 up to 0.5. Thus, this proves that both wavelet LMMSE and NLM filters are excellent at removing noise with respect to PSNR evaluation. This is then followed by Lee filter and then SRAD with average to moderate PSNR values.

USDSAI evaluates how well the filter reduces the variances of homogenous regions while having the ability to keep the different classes of regions well separated. When the classes are well separated then the numerator in (9) will be large and if the intraclass variances are small, the denominator in (9) will be small in which both cases result in high value of USDSAI. From Table II it can be seen that for Lena image NLM filter has the highest USDSAI values, however with slight inconsistency at noise variances 0.4 and 0.5. This is also unanimous with the results when Barbara and Boat image are used. In both the results using Barbara and Boat images, NLM filter is observed to have the highest USDSAI values. We can conclude that it is the outperforming filter in terms of USDSAI evaluation. Therefore this indicates that NLM filter produces the most desirable image restoration with the ability to preserve image contrast and at the same time is superior at speckle removal. This is then followed by Lee, wavelet LMMSE and SRAD filters.

TABLE I: Comparison of PSNR values on speckled images

Lena					
Noise variance	Noisy	SRAD	Lee	LMMSE	NLM
0.04	27.20	24.33	26.11	28.58	27.75
0.06	25.44	22.66	25.94	28.70	27.64
0.08	24.18	21.03	25.78	28.76	27.54
0.1	23.22	19.30	25.66	28.67	27.39
0.2	20.22	16.41	25.13	28.08	26.57
0.3	18.47	14.07	24.71	27.02	25.59
0.4	17.19	13.54	23.70	24.32	23.20
0.5	16.24	12.62	23.19	22.47	21.83
Barbara					
Noise variance	Noisy	SRAD	Lee	LMMSE	NLM
0.04	25.99	18.74	23.22	24.53	25.29
0.06	24.24	17.61	23.08	24.58	25.22
0.08	22.95	16.01	22.92	24.63	25.09
0.1	22.04	15.48	22.70	24.67	25.01
0.2	18.99	13.60	22.16	24.46	23.95
0.3	17.24	13.27	21.63	23.69	22.54
0.4	15.99	10.84	21.14	22.33	21.09
0.5	15.02	10.80	20.68	20.84	19.72
Boat					
Noise variance	Noisy	SRAD	Lee	LMMSE	NLM
0.04	25.41	21.61	22.11	24.40	24.33
0.06	23.65	20.34	22.11	24.74	24.31
0.08	22.42	18.44	22.0	24.77	24.30
0.1	21.44	16.96	21.87	24.79	24.25
0.2	18.44	14.08	21.36	24.67	23.64
0.3	16.67	12.75	20.89	23.80	22.42
0.4	15.44	11.54	20.45	22.35	21.40
0.5	14.47	10.67	20.07	20.72	19.71

TABLE II: Comparison of USDSAI values on speckled images

Lena						
Noise variance	Original	Noisy	SRAD	Lee	LMMSE	NLM
0.04	1	0.89	1.06	1.30	1.27	1.52
0.06	1	0.81	1.04	1.25	1.21	1.46
0.08	1	0.76	0.98	1.19	1.15	1.43
0.1	1	0.79	1.07	1.32	1.26	1.52
0.2	1	0.60	1.39	1.20	1.18	1.44
0.3	1	0.55	1.26	1.22	1.10	1.35
0.4	1	0.43	1.32	1.14	0.95	1.28
0.5	1	0.36	0.79	0.93	0.72	0.92
Barbara						
Noise variance	Original	Noisy	SRAD	Lee	LMMSE	NLM
0.04	1	0.93	1.07	1.38	1.12	1.64
0.06	1	0.84	0.96	1.28	1.08	1.56
0.08	1	0.79	0.87	1.24	1.06	1.50
0.1	1	0.71	0.84	1.17	0.99	1.46
0.2	1	0.71	0.91	1.38	1.22	1.57
0.3	1	0.52	0.70	1.04	0.88	1.18
0.4	1	0.55	0.70	1.34	1.08	1.49
0.5	1	0.44	0.79	1.08	0.83	1.15
Boat						
Noise variance	Original	Noisy	SRAD	Lee	LMMSE	NLM
0.04	1	0.87	1.01	1.44	1.26	1.70
0.06	1	0.75	1.11	1.27	1.14	1.61
0.08	1	0.83	1.28	1.44	1.29	1.79
0.1	1	0.74	1.16	1.34	1.19	1.67
0.2	1	0.69	1.14	1.52	1.39	1.66
0.3	1	0.54	1.09	1.37	1.22	1.59
0.4	1	0.49	1.05	1.14	1.02	1.24
0.5	1	0.37	1.04	1.06	0.84	1.10



Figure 1: Lena images with noise variance 0.1. (a) Noise-free image (b) Noisy image (c) SRAD Filter (d) Lee Filter (e) LMMSE Filter (f) NLM Filter

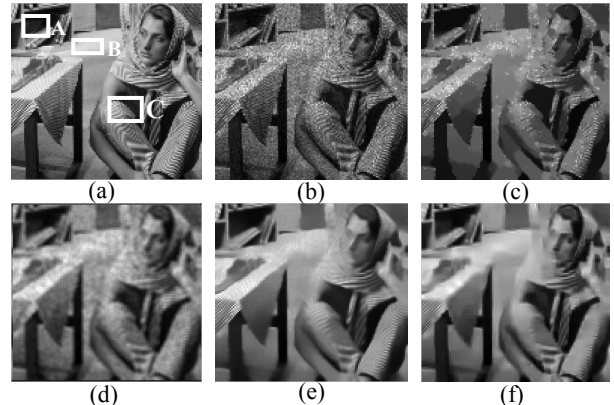


Figure 2: Barbara images with noise variance 0.1. (a) Noise-free image (b) Noisy image (c) SRAD Filter (d) Lee Filter (e) LMMSE Filter (f) NLM Filter

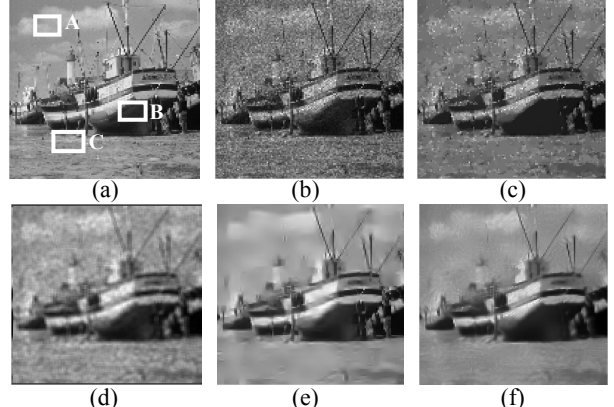


Figure 3: Boat images with noise variance 0.1. (a) Noise-free image (b) Noisy image (c) SRAD Filter (d) Lee Filter (e) LMMSE Filter (f) NLM Filter

Generally, in terms of visual inspection, SRAD filter does not result in over-smoothing and hence does not cause blurring. However, it can be observed that there are still a lot of speckle retained in the image. This is evident from Figs. 1(c), 2(c) and 3(c). Lee filter utilized in this experiment is of window size 3 by 3 and it performs well in terms of noise removal whereby almost 70% of the speckle noise is removed. However the filtering results in blurring effect and failure in preserving the

edges as well as important features of the image. This is clearly depicted through Figs. 1(d), 2(d) and 3(d). Wavelet (LMMSE) performs extremely well in removing the speckle noise which can be analyzed in Fig. 1(e), 2(e) and 3(e) whereby the image seems almost clear from noise and just minimal noise left. It does result in blurring to some degree though much less compared to Lee filter. NLM filter also did a good job in terms of speckle noise suppression however it is observed in Figs. 1(f), 2(f) and 3(f) to cause more blurring than wavelet (LMMSE) filter.

Through visual analysis the filters that are best at removing speckle noises are NLM and wavelet LMMSE filter. NLM and LMMSE filters both results in denoised images of almost the same quality. Both filters are excellent in terms of speckle removal as it is proven from Fig. 3(e) and (f) that most of the speckle are removed. However the denoised images' background is still in darker tone which is distinct from the background of noise-free image. In comparison to NLM filter, wavelet LMMSE filter tends to over-smooth the image slightly. Lee filter manage to denoise the noise-corrupted image to an extent that it has lighter background color as depicted in Figure 3(c). However the image restored is blurry and there are some losses of image details and textures. Besides, it can also be observed that some noises are still retained in the denoised image by Lee filter. The image denoised by SRAD filter shows just a slight improvement from the artificially noise speckled image. It removes some speckle noise but most of the speckle noises are still retained in the denoised image.

B. Using Field II Simulated Image

In this part of experiment, a cyst resembling phantom image is generated using the MATLAB Field II simulation version 3.2. The phantom consists of five point targets; 6, 5, 4, 3, and 2 mm diameter water-filled cysts, along with 6, 5, 4, 3, and 2 mm diameter high scattering regions. The original cyst phantom in Fig. 4(a) is composed of 3 constant classes and the filters' ability to reduce speckle noise while keeping the distinct classes well separated will be evaluated using normalized variance, mean preservation, and USDSAI assessment.

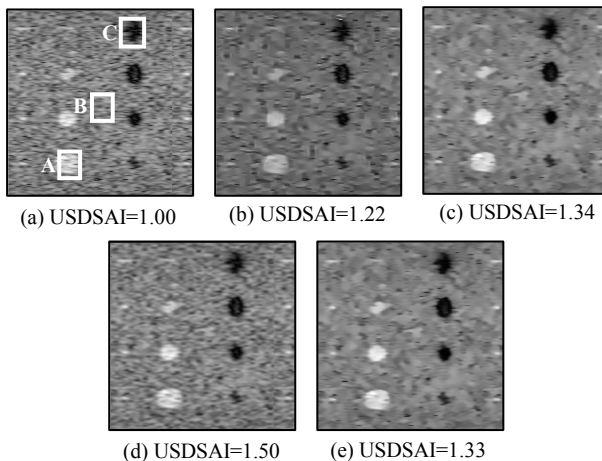


Figure 4: Field II Simulated Image, Cyst Phantom with USDSAI values (a) original (b) wavelet LMMSE filter (c) Lee filter (d) NLM filter (e) SRAD filter

TABLE III: Normalized variance for restored images in Fig. 9

Regions	Original	SRAD	Lee	LMMSE	NLM
A	0.0473	0.0364	0.0359	0.0362	0.0359
B	0.0417	0.0200	0.0259	0.0292	0.0140

TABLE IV: Mean Preservation for restored images in Fig. 9

Regions	Original	SRAD	Lee	LMMSE	NLM
A	178.34	0.70	178.40	177.38	178.32
B	128.27	0.50	128.19	127.02	129.71

Fig. 4 shows the restored images along with the USDSAI values. The results for normalized variance and mean preservation can be analyzed in Table III and Table IV respectively. The three regions A, B and C selected for the USDSAI evaluation are shown in Fig. 4(a). The USDSAI values for each filter are shown together with the denoised images in Figs. 4 (b), (c), (d) and (e). The normalized variance and mean preservation are calculated over two regions and in this report the regions used are region A and region B. From the result obtained for USDSAI evaluation the highest USDSAI value achieved is 1.50 by NLM filter. This is followed by Lee, SRAD and then wavelet LMMSE. However all the restored images are improved in terms of contrast level since all of them have USDSAI values greater than 1. Therefore for Field II simulated image, NLM filter is proven to be better and produces more desirable image restoration.

Normalized variance and mean preservation of the original cyst phantom image are calculated and compared to the normalized variance and mean preservation of all restored images by each filter and presented in Table III and IV. The reduction of normalized variance in denoised image indicates better noise reduction by the filter. From Table III it is evident that NLM filter results in lowest normalized variance in both region A and B hence indicating high level of noise reduction. This is followed by Lee, SRAD and wavelet LMMSE. Through mean preservation aspect, for region A it is observed in Table IV that NLM is best at preserving mean as the restored image by this filter has closest mean to the original image's mean. However for region B, Lee is seen with closest mean value to the original image's mean value. This is probably due to the nature of Lee filter that is based on averaging technique hence it has the tendency to retain the mean of original image.

Through visual inspection, the restored image by wavelet LMMSE filter in Fig. 4(b) are much less noisy than the original however it suffers some loss in details and textures as the filter tends to smooth the image. Lee filter reduces speckle noises but it causes blurring effect to the denoised image making it difficult to be analyzed. NLM filter performs best for Field II simulated image since it is excellent at removing noise and still manages to maintain the image details, textures and enhances contrast as confirmed by its highest USDSAI value. The restored image by SRAD is over-smoothed and the image details and textures are lost.

C. Using Real Ultrasound Image

In this part of experiment, the performances of the filters are analyzed using real ultrasound images captured from

patients. The images used are malignant and benign tumors. The image size is 1536×256 pixels. The patient with

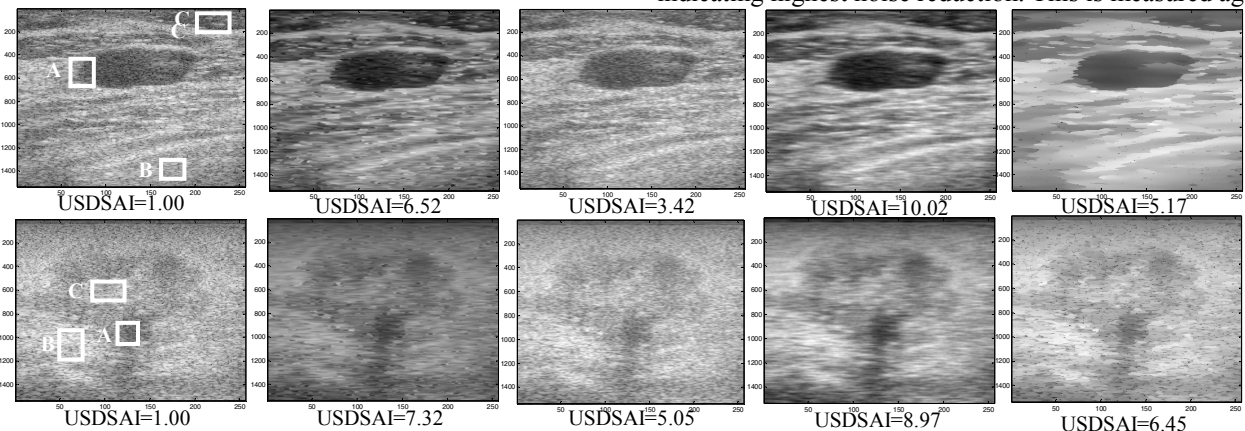


Figure 5: Restoration of benign tumor (top) and malignant tumor (bottom) from left to right, Original, wavelet LMMSE filter, Lee filter, NLM filter and SRAD filter.

malignant tumor was diagnosed with IDC (Invasive Ductal Carcinoma) and the patient with benign tumor was diagnosed with fibroadenoma. The RF frames are recorded at 17 frame/second and a total of 12 seconds of data are obtained using a linear transducer array from the Antares ® System. The URI Offline Processing Tools (URI-OPT) run on MATLAB platform is used to convert the RF data to the B-mode images as shown in Figs. 5. The performances of filters in denoising real US images are evaluated through USDSAI, mean preservation and normalized variance. For USDSAI assessment to be carried out, three regions are selected regions A, B and C for both benign and malignant tumor image. The restored images are depicted in Figs. 5 along with the USDSAI results. The mean preservation and normalized variance are evaluated over two homogenous areas. The homogenous areas selected for benign tumor image are the corresponding regions A and C selected for USDSAI evaluation. Meanwhile for malignant tumor image, the homogenous areas chosen for mean preservation and normalized variance assessment are the corresponding regions A and B selected for USDSAI evaluation. Normalized variance and mean preservation results are presented in Table V and VI.

TABLE V: Normalized Variance for restored images in Fig. 5

Benign Tumor	Original	SRAD	Lee	LMMSE	NLM
Region A	0.034	0.0039	0.0082	0.0040	0.0025
Region C	0.018	0.0048	0.012	0.0077	0.0044
Malignant Tumor	Original	SRAD	Lee	LMMSE	NLM
Region A	0.013	0.013	0.0067	0.0035	0.0021
Region B	0.0070	0.0097	0.0066	0.0039	0.0027

TABLE VI: Mean Preservation for restored images in Fig. 5

Benign Tumor	Original	SRAD	Lee	LMMSE	NLM
Region A	5.66	0.37	4.83	4.80	4.84
Region C	5.27	0.43	5.23	5.21	5.24
Malignant Tumor	Original	SRAD	Lee	LMMSE	NLM
Region A	6.90	0.47	5.29	5.27	5.32
Region B	7.18	0.80	7.49	7.49	7.47

From the results tabulated in Table V it is evident that the image denoised by NLM filter has lowest normalized variance indicating highest noise reduction. This is measured against

the normalized variance of the original image before being denoised. This result is unanimous between both benign and malignant tumor images. As for benign tumor image the next best noise reducing filter is SRAD followed by wavelet LMMSE and Lee filter. Meanwhile, for malignant tumor image the next best noise reducing filter after NLM filter is wavelet LMMSE, followed by Lee and SRAD.

Table VI shows the tabulated data of mean preservation for benign and malignant tumor images. It is shown that NLM filter results in mean value nearest to the mean value of original image before being denoised. This is then followed by Lee, wavelet LMMSE and SRAD. This is unanimous for both the benign and malignant tumor images.

Figs. 5 show the restored benign and malignant tumor images together with their corresponding USDSAI values. It is clearly shown from Fig. 5 that wavelet LMMSE has significantly reduced noise while maintaining most of the image details. This is also supported by its high value of USDSAI. However the highest USDSAI value is found to be from the image denoised by NLM filter. Through visual inspection though, the image restoration by NLM filter is slightly blurry compared to the image filtered by wavelet LMMSE. Nevertheless, the higher USDSAI value by NLM filter proves that it produces most desirable image restoration. SRAD filter produces over-smoothed image and Lee filter performs averagely in terms of USDSAI evaluation.

The processing times for each filter are also calculated and compared in Table VII. The time is measured in seconds.

TABLE VII: Processing time for each filter

	SRAD	Lee	LMMSE	NLM
Benign Tumor	63.98	82.33	65.99	671.66
Malignant Tumor	63.73	81.31	69.81	642.82

The filter with fastest processing time is SRAD filter which is then followed by wavelet LMMSE filter. Wavelet LMMSE is just slightly slower than SRAD. Lee filter has moderate

processing time which is slower when compared to SRAD and wavelet LMMSE. NLM filter has the slowest processing time which is approximately 10 times the processing time for SRAD and wavelet LMMSE.

V. CONCLUSIONS

This study focuses on the evaluation of the selected filters in terms of speckle noise suppression and texture preservation. The conducted experiments involved simulated speckled noise images, computer generated images and real US images. Using simulated data it is found that the wavelet LMMSE filter performs best in noise suppression as proven through PSNR assessment whereas NLM filter is the second best filter in terms of PSNR evaluation and it is as good as wavelet LMMSE filter. NLM filter is also competent in terms of producing desirable image restoration and this is proven through its USDSAI values. Using computer generated data and real ultrasound data, the NLM filter outperforms others in terms of USDSAI, mean preservation and normalized variance assessments. The processing time of NLM filter is the longest which is approximately 10 times the processing time for SRAD and wavelet LMMSE filters. The filter with next best performance but with faster processing time is wavelet LMMSE. It is concluded that NLM filter is the best filter in all scenarios considering both speckle noise suppression and image texture preservation.

ACKNOWLEDGEMENT

The authors would like to thank Universiti Teknologi PETRONAS for providing financial support.

REFERENCES

- [1] C.P. Loizou and C.S. Pattichis "Introduction to Ultrasound Imaging and Speckle Noise," in Despeckle Filtering Algorithms and Software for Ultrasound Imaging, Morgan & Claypool Publishers, 2008, pp. 3-23.
- [2] I. Elamvazuthi M.L. Muhd Zain and K.M. Begam, "Despeckling of ultrasound images of bone fracture using multiple filtering algorithms" SciVerse ScienceDirect Mathematical and Computer Modelling, vol. 57, pp. 152-168, 2013.
- [3] E. Nadernejad, "Despeckle filtering in medical ultrasound imaging", Contemp. Eng. Sci., vol. 2, no. 1, pp. 17-36, 2009.
- [4] S. Sudha, G.R. Suresh, R. Sukanesh, "Speckle noise reduction in ultrasound images by wavelet thresholding based on weighted variance", Int. J. Comput. Theory Eng., vol. 1, no. 1, pp. 7-12, 2009.
- [5] J.S. Lee, "Refined filtering of image noise using local statistics," Computer Vision, Graphics and Image Processing, vol.15, pp. 380-389, 1981.
- [6] D. T. Kuan, A.A. Sawchuck, T.C. Strand, and P. Chavel, "Adaptive restoration of images with speckle," IEEE Trans. Acoustics, Speech and Signal Processing, vol. 1, no. 3, pp. 373-383, 1987.
- [7] A. Loper, "Adaptive speckle filters and scene heterogeneity," IEEE Trans. Geoscience and Remote Sensing, vol. 28, no.6, pp. 992-1000, Nov.1990.
- [8] S. Solbo and T. Eltoft, "Homomorphic wavelet based-statistical despeckling of SAR images," IEEE Trans. Geosci. Remote Sens., vol. 42, no. 4, pp. 711-721, 2004.
- [9] R. Perona and J. Malik, "Scale-space and edge detection using anisotropic diffusion," IEEE Trans. Pattern Anal. Mach. Intell., vol.12, no.7, pp. 629- 639, July 1990.
- [10] Y. Yongjian and S.T. Acton, "Speckle reducing anisotropic diffusion." IEEE Trans. Image Process, vol. 11, no. 11, pp. 1260-1270, Nov. 2002.
- [11] L. Zhang, P. Bao, and X. Wu, "Multiscale LMMSE-Based Image Denoising With Optimal Wavelet Selection" IEEE Trans. Circuits and Systems For Video Technology, vol. 15, No. 4, pp. 469-481, April 2005.
- [12] A. Buades, B. Coll, and J. M. Morel, "Image Denoising By Non-Local Averaging" in Computer Vision and Pattern Recognition, 2005. CVPR 2005. IEEE Computer Society Conference, vol. 2, pp. 60-65, 2005.
- [13] T. Joel and R. Sivakumar, "Despeckling of Ultrasound Medical Images: A Survey" in Journal of Image and Graphics, vol. 1, no. 3, pp. 161-164, Sept. 2013.
- [14] L. Zhang and P. Bao, "Edge detection by scale multiplication in wavelet domain," Pattern Recognit. Lett., vol. 23, pp. 1771-1784, 2002.
- [15] S. G. Chang, B. Yu, and M. Vetterli, "Adaptive wavelet thresholding for image denoising and compression," IEEE Trans. Image Process., vol. 9,no.9, pp. 1532-1546, Sep. 2000.
- [16] G. Fan and X. G. Xia, "Improved hidden Markov models in the wavelet-domain,"IEEE Trans. Signal Process., vol. 49, no. 1, pp. 115-120, Jan 2001.
- [17] Y. Cui, T. Zhang, S. Xu and W. Yu, "Image Despeckling Based on LMMSE Wavelet Shrinkage", Dalian Nationalities University Electrical Review, pp. 269-272, 2012.
- [18] W. Chen, M. Ding, Y. Miao, and L. Luo, "Ultrasound image denoising with multi-shape patches aggregation based non-local means" International Conference on Intelligent Computation and Bio-Medical Instrumentation, pp. 35-38, 2011.
- [19] V. Karnati, M. Uliyar, and S. Dey "Fast non-local algorithm for image denoising," in Proc. of IEEE ICIP, Cairo, Egypt, 2009.
- [20] R. Sivakumar, M.K. Gayathri and D. Nedumaran, "Speckle Filtering Of Ultrasound B-Scan Images-A Comparative Study Between Spatial And Diffusion Filters", IEEE Conference on Open Systems (ICOS 2010), December 2010.
- [21] P.C. Tay et al., "Ultrasound Despeckling for Contrast Enhancement" IEEE Trans. Image Processing, vol. 19, no. 7, pp. 1847-1860, July 2010.
- [22] S. Finn, M. Glavin and E. Jones, "Echocardiographic Speckle Reduction Comparison." IEEE Trans. Ultrasonics, Ferroelectrics and Frequency Control, vol.58, no. 1, pp. 82-101, Jan. 2011.
- [23] S. Wu, Q. Zhu, and Y. Xie, "Evaluation of various speckle reduction filters on medical Ultrasound images" 35th Annual International Conference of the IEEE EMBS, pp. 1148-1150, July 2013.
- [24] R. Ma, X. Zhang and M. Ding, "Quantitative Study on Despeckle Methods of Medical Ultrasound Images" International Conference on Intelligent Computation and Bio-Medical Instrumentation, pp. 120-123, 2011.
- [25] N. Yahya, Nidal S. Kamel, Aamir S. Malik, *Subspace-based Technique for Speckle Noise Reduction in SAR Images*, IEEE Transactions on Geoscience and Remote Sensing., vol. 52, no. 10, pp. 6257-6271, Oct 2014.